A HIGH-PRECISION MODELING FOR WORKPIECES BASED ON ALIGNED LINES AND THE FORECASTING OF CUTTING MARKS IN NC SIMULATION

Zhongxu TIAN[1], Ye YUAN[2]

In numerically controlled (NC) machining simulation, the surfaces of workpieces are usually expressed with aligned-lines perpendicular to an xy- plane to avoid time-consuming Boolean operation. Since the swept surfaces are usually represented analytically, the derivatives with respect to x and y can be calculated easily. Based on aligned-line scheme, a new scheme is presented, which uses the derivatives to improve the description precision of the workpieces surfaces. The cutting marks can also be found out in the new scheme. Two instances show that the time cost for computation increases a little more but the simulation precision can be improved significantly.

Keywords: NC Machining; Aligned-lines; High Precision; Derivative; Cutting Mark.

1. Introduction

Computational simulations are widely used in analyzing tool paths in NC machining [1-6]. It can not only simulate the cutting processes but also evaluate the cutting performance. Both efficiency and accuracy are required in NC simulation.

The models for workpieces generally include discrete models and solid-based models. Many discrete models, e.g., Z-map [7], Z-buffer [8], G-buffer [9], ray casting [10] etc., are implemented in machining applications. In most of the methods, aligned lines are used to represent the workpieces to avoid time-consuming Boolean operation existing in solid models. But the simulation accuracy depends on the density of the aligned lines. When high accuracy is desired, the computational cost becomes a concern.

In the aligned-line scheme, the workpiece is approximated by a set of aligned lines passing through the grid points on a xy-plane [7]. The machining process is simulated through updating the lengths of the lines or the heights with

[1] Institute of Technology, Shanghai Ocean University, Shanghai 201306, China E-mail: zxtian@shou.edu.cn.
[2] School of Statistics and Information, Shanghai University of International Business and Economics, Shanghai 201620, China. E-mail: aaaayuanye@126.com.

respect to xy-plane after calculating the intersection points between the tool's swept surface and aligned lines.

The calculating complexity of the tool's swept surface depends on the tool's shape and movements. Numerous researches focused on deriving the swept surfaces of various tools with various movements [11-15]. Accuracy is the main measurement of the algorithms' performance. The algorithms such as positioning movement error compensation, linear interpolation movement, and circular interpolation movement error compensation are used for error compensation purpose [16], and NC program is reconstructed according to the predicted errors during virtual machining. The results show that error compensation methods via reconstructing NC programs can notably improve the tools' movement accuracy. A mechanistic model for cutting force prediction is proposed by Femandez-Abia [17]. This model was developed for machining with nose radius tools considering the effect of the edge force due to the rounded cutting edge. The analysis of the results shows that the material undergoes a significant change in its behavior when machining at cutting speeds over 0.0075m/s, which favors the machining operation. The main component of cutting forces reaches a minimum value at this cutting speed. A model for the prediction of the cutting forces when turning austenitic stainless steels following the approach of mechanistic models is presented by Ana Isabel Femandez-Abia [18]. This model provides an estimation of the cutting forces with a reasonable precision. It can be used in the machine-tools and fixtures design or the optimization of cutting tool geometry. The swept surfaces are usually analytically expressed by explicit or implicit formulas, and the derivatives of the height functions with respect to x and y can also be calculated easily. They both may be used to improve the precision of modeling for workpieces. In this paper, a new scheme using the derivatives is presented to express the workpieces with higher precision without much increment in calculation cost and the cutting marks of the workpieces can also be found out with this scheme.

This paper is organized as follows: Section 2 gives the modeling of the workpiece surfaces by borrowing the derivatives of height functions. Section 3 presents the computational method of the cutting marks. In section 4, the swept surfaces of ball-end tools and the derivatives of them are derived as well. Section 5 illustrates valuation method for the precision of the schemes. Finally in section 6, two instances are given to investigate the precision of the new scheme with respect to Z-map scheme.

2. Modeling for Workpieces Surfaces

In Fig.1, the surfaces of a workpiece are composed of many small smooth surfaces, which can be expressed in height-function forms with respect to

xy-plane. The plane is meshed and described by many nodes and the height function near an arbitrary node, i, can be expressed in the following forms:

$$w_i(x,y) \approx w_i + \left(\frac{\partial w}{\partial x}\right)_i (x-x_i) + \left(\frac{\partial w}{\partial y}\right)_i (y-y_i) + \frac{1}{2}\left(\frac{\partial^2 w}{\partial x^2}\right)_i (x-x_i)^2 + \\ + \left(\frac{\partial^2 w}{\partial x \partial y}\right)_i (x-x_i)(y-y_i) + \frac{1}{2}\left(\frac{\partial^2 w}{\partial y^2}\right)_i (y-y_i)^2 \quad , \qquad (1)$$

where $(\ )_i$ are the derivatives values at node i.

In a four-node element (shaded domain in Fig.1), determined by nodes i, j, k and m, the final surface of the workpiece can be expressed in the following form, when it is viewed from above:

$$w(x,y) = \min\left(w_i(x,y), w_j(x,y), w_k(x,y), w_m(x,y)\right) \qquad (2)$$

Comparing with other aligned-line based methods, the new method does the calculations of w, $\partial w/\partial x$, $\partial w/\partial y$, $\partial^2 w/\partial x^2$, $\partial^2 w/\partial x \partial y$, $\partial^2 w/\partial y^2$ at every node. Since the swept surfaces of the cutter are usually expressed analytically, the abovementioned nodal parameters can be computed conveniently, and the formulae for ball-end cutters are given to investigate the new scheme in section 4.

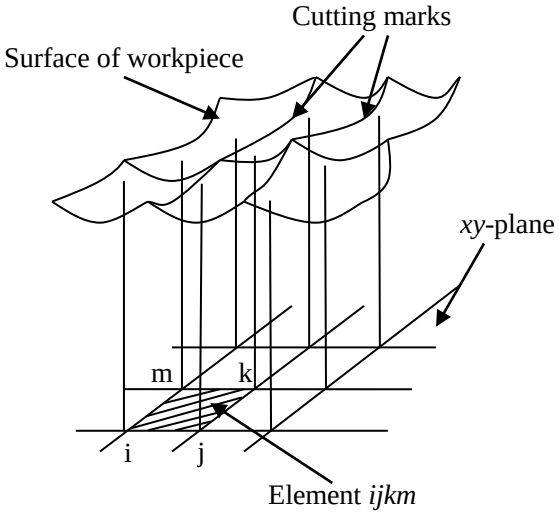

Fig. 1. Aligned-line based method

3. Computation of Cutting Mark

As the surfaces of workpieces can be expressed in more detailed forms in the new scheme, cutting marks can be presented with the following method.

Suppose xy- plane is meshed densely enough, and there is at most one cutting mark between any two neighboring nodes. All the possible cutting-mark elements are shown in Fig.2 and Fig.3.

In order to reduce the computation, the cutting-mark elements should be selected out in the first place.

For any two neighboring nodes, i and j, the following formula could be satisfied if there is a cutting mark between them:

$$\left|w_i(x_i,y_i)-w_j(x_i,y_i)\right|+\left|w_i(x_j,y_j)-w_j(x_j,y_j)\right|>r \tag{3}$$

where function $w_i(x,y)$ and $w_j(x,y)$ are defined as shown in (2).

Formula (3) indicates that the height results of node i and j, which are calculated with $w_i(x,y)$and $w_j(x,y)$, are far enough and node i and j lie in different patches. That is, $w_i(x,y)$ and $w_j(x,y)$ are different patch functions and there must be a cutting mark between them.

There are two terms on the left side of the formula (3), which are to consider the cutting marks near node i and j, respectively.

After the cutting marks elements are identified, the points lying on cutting marks can be found out by using the following characters.

Any point, $Q(x_Q,y_Q)$, on cutting marks should have the following characteristics:

Characteristic 1: There should be at least two nodal functions, $w_i(x,y)$ and $w_j(x,y)$, whose values on the cutting marks are very close, and can be expressed as

$$\left|w_i(x_Q,y_Q)-w_j(x_Q,y_Q)\right|<t_1 \tag{4}$$

where t_1 is a small constant.

Characteristic 2: The derivatives determined by $w_i(x,y)$ and $w_j(x,y)$ are different enough, which can be presented by

$$\left|\left.\frac{\partial w_i(x,y)}{\partial x}\right|_{(x_Q,y_Q)}-\left.\frac{\partial w_j(x,y)}{\partial x}\right|_{(x_Q,y_Q)}\right|+\left|\left.\frac{\partial w_i(x,y)}{\partial y}\right|_{(x_Q,y_Q)}-\left.\frac{\partial w_j(x,y)}{\partial y}\right|_{(x_Q,y_Q)}\right|>t_2 \tag{5}$$

where t_2 is a relatively large constant.

Using the given characteristic 1 and 2, the points on cutting marks can be identified in every element.

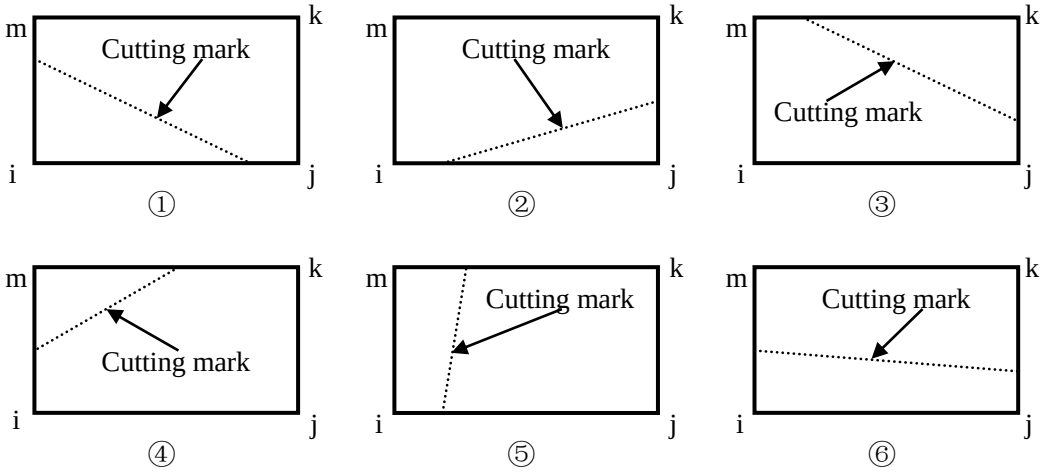

Fig. 2. Cutting mark in element without intersections (Only one mark in an element)

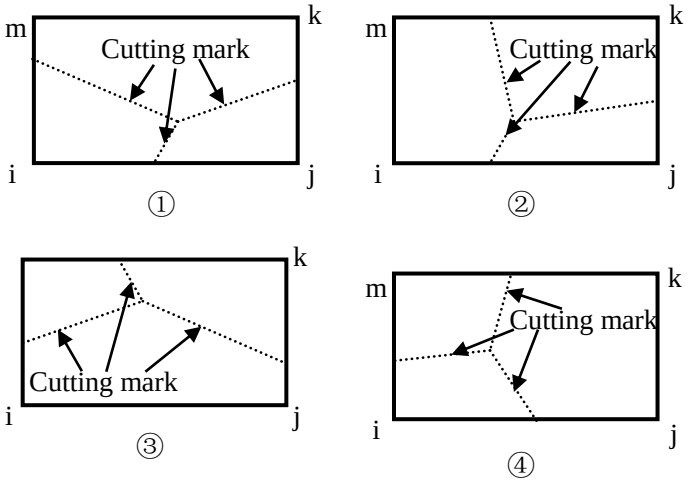

Fig. 3. Cutting marks in element with intersections (More marks in an element)

4. Computation of Nodal Parameters for Ball-end Tools

Since the swept surface model of the ball-end tools is simple, we take it as an example to investigate the new scheme for workpieces.

The movement of ball-end tools composes of many small movements along straight paths. As the roads become shorter, the swept surfaces can be expressed with higher precision. The swept surfaces of ball-end tools can be divided into several sub-domains, which can be expressed analytically, piecewise.

In Fig.4, the center of the ball-end cutter moves from position $A(x_A, y_A, z_A)$ to position B (x_B, y_B, z_B), along a straight road. In this instance, the sub-domains are the start-domain, the mid-domain, and the end-domain. They match the start-surface, the mid-surface and the end-surface of the swept surface. The following section shows the height functions of the swept surfaces in these three sub-domains.

The start-surface and the end-surface are all spherical surfaces with radius r, and can be expressed as:

$$\begin{cases} (x-x_A)^2+(y-y_A)^2+(z-z_A)^2=r^2 & in\ start-domain \\ (x-x_B)^2+(y-y_B)^2+(z-z_B)^2=r^2 & in\ end-domain \end{cases}. \tag{6}$$

And the height functions can be given in the following forms:

$$\begin{cases} z=z_A-\sqrt{r^2-(x-x_A)^2-(y-y_A)^2} & in\ start-domain \\ z=z_B-\sqrt{r^2-(x-x_B)^2-(y-y_B)^2} & in\ end-domain \end{cases}. \tag{7}$$

The directional derivatives of the start-surface are:

$$\frac{\partial z}{\partial x}=-\frac{x-x_A}{z-z_A} \qquad \frac{\partial z}{\partial y}=-\frac{y-y_A}{z-z_A}$$

$$\frac{\partial^2 z}{\partial x^2}=-\frac{1+\left(\frac{\partial z}{\partial x}\right)^2}{z-z_A} \qquad \frac{\partial^2 z}{\partial x\partial y}=-\frac{\frac{\partial z}{\partial x}\frac{\partial z}{\partial y}}{z-z_A} \qquad \frac{\partial^2 z}{\partial y^2}=-\frac{1+\left(\frac{\partial z}{\partial y}\right)^2}{z-z_A}. \tag{8}$$

and those of the end-surface are:

$$\frac{\partial Z}{\partial X}=-\frac{X-X_B}{Z-Z_B}, \qquad \frac{\partial Z}{\partial y}=-\frac{y-y_B}{Z-Z_B},$$

$$\frac{\partial^2 Z}{\partial X^2}=-\frac{1+\left(\frac{\partial Z}{\partial X}\right)^2}{Z-Z_B}, \frac{\partial^2 Z}{\partial x\partial y}=-\frac{\frac{\partial Z}{\partial X}\frac{\partial Z}{\partial y}}{Z-Z_B}, \frac{\partial^2 Z}{\partial y^2}=-\frac{1+\left(\frac{\partial Z}{\partial y}\right)^2}{Z-Z_B}. \tag{9}$$

The mid-surface is a cylindrical surface, whose axis can be described with the following unit vector:

$$\mathbf{r_{AB}}=\frac{\mathbf{r_B}-\mathbf{r_A}}{L_{AB}}=\{k_1 \quad k_2 \quad k_3\}^T, \tag{10}$$

where,

$$\mathbf{r}_A=\{x_A \quad y_A \quad z_A\}^T, \quad \mathbf{r}_B=\{x_B \quad y_B \quad z_B\}^T,$$

$$L_{AB} = \sqrt{(x_B - x_A)^2 + (y_B - y_A)^2 + (z_B - z_A)^2} \ ,$$

$$k_1 = \frac{x_B - x_A}{L_{AB}} \quad , \qquad k_2 = \frac{y_B - y_A}{L_{AB}}, \quad k_3 = \frac{z_B - z_A}{L_{AB}} .$$

For any point $P(x, y, z)$ attached to the mid-surface, the distance to the axis is

$$\left\| \vec{AP} \times \vec{AB} \right\| = r \tag{11}$$

So, the mid-surface can be expressed in the following equation:

$$Az^2 + Bz + C = 0 \ , \tag{12}$$

where,

$$A = k_1^2 + k_2^2,$$

$$B = -2k_1k_3(x - x_A) - 2k_2k_3(y - y_a) - 2(k_1^2 + k_2^2)z_a ,$$

$$C = (k_3(y - y_a) + k_2 z_a)^2 + (k_2(x - x_a) - k_1(y - y_a))^2 + (-k_1 z_a - k_3(x - x_a))^2 - r^2$$

Per equation (9), the height in mid-domain can be expressed by

$$z = \frac{-B - \sqrt{B^2 - 4AC}}{2A} \quad . \tag{13}$$

For the mid-surface, the directional derivatives can be derived from equation (12), shown below:

$$\begin{aligned} &\frac{\partial z}{\partial x} = -\frac{C_2}{C_1}, \frac{\partial z}{\partial y} = -\frac{C_3}{C_1}, \frac{\partial^2 z}{\partial x^2} = -\frac{1}{C_1}\left(\frac{\partial C_2}{\partial x} - \frac{C_2}{C_1}\frac{\partial C_1}{\partial x}\right), \\ &\frac{\partial^2 z}{\partial x \partial y} = -\frac{1}{C_1}\left(\frac{\partial C_2}{\partial y} - \frac{C_2}{C_1}\frac{\partial C_1}{\partial y}\right), \frac{\partial^2 z}{\partial y^2} = -\frac{1}{C_1}\left(\frac{\partial C_3}{\partial y} - \frac{C_3}{C_1}\frac{\partial C_1}{\partial y}\right), \end{aligned} \tag{14}$$

where,

$$C_1 = -k_2k_3(y - y_A) + (k_1^2 + k_2^2)(z - z_A) - k_1k_3(x - x_A),$$

$$C_2 = -k_1k_3(z - z_A) + (k_2^2 + k_3^2)(x - x_A) - k_1k_2(y - y_A),$$

$$C_3 = -k_2k_3(z - z_A) + (k_1^2 + k_3^2)(y - y_A) - k_1k_2(x - x_A),$$

$$\frac{\partial C_1}{\partial x} = (k_1^2 + k_2^2)\frac{\partial z}{\partial x} - k_1k_3 , \qquad \frac{\partial C_1}{\partial y} = (k_1^2 + k_2^2)\frac{\partial z}{\partial y} - k_2k_3 ,$$

$$\frac{\partial C_2}{\partial x} = -k_1 k_3 \frac{\partial z}{\partial x} + k_2^2 + k_3^2, \qquad \frac{\partial C_2}{\partial y} = -k_1 k_3 \frac{\partial z}{\partial y} - k_1 k_2,$$

$$\frac{\partial C_3}{\partial x} = -k_2 k_3 \frac{\partial z}{\partial x} - k_1 k_2, \qquad \frac{\partial C_3}{\partial y} = -k_2 k_3 \frac{\partial z}{\partial y} + k_1^2 + k_3^2.$$

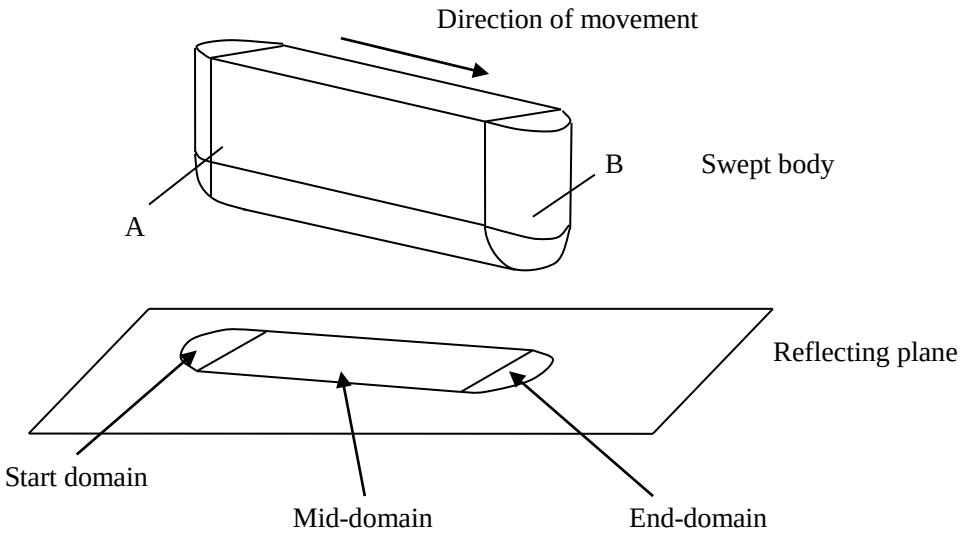

Fig. 4. Swept surface and reflection domain

5. Valuation of the Precision

The surface in the shaded domain in Fig.1 is described with nodal parameters of node i, j, k and m, which can be computed with formula (1). When we focus on the simulation process, fewer additional nodes in element ijkm are needed to describe the surface in the shaded domain. But when we focus on the error investigations of the machining, more additional nodes are needed instead.

Here, we use the internal height in every element to investigate the precision of the new scheme compared with Z- map scheme. The error can be computed with the following formula:

$$error = \left| w - w_e \right|. \tag{15}$$

Where, w is the height from simulation, while w_e is the exact height. For the new scheme given in this paper, height w can be calculated by formula (1). For Z-map scheme, the height w is calculated through bi-linear interpolation, which is well known in finite element method and can be expressed as:

$$w = \frac{1}{4}(1-\xi)(1-\eta)w_i + \frac{1}{4}(1+\xi)(1-\eta)w_j + \frac{1}{4}(1+\xi)(1+\eta)w_k + \frac{1}{4}(1-\xi)(1+\eta)w_m \quad , \tag{16}$$

where,

$$\begin{cases} \xi = \dfrac{(x - x_C)}{a} \\ \eta = \dfrac{(y - y_C)}{b} \end{cases} \qquad x_C = \frac{x_i + x_j + x_k + x_m}{2} \qquad y_C = \frac{y_i + y_j + y_k + y_m}{2}$$

$$a = |x_i - x_C| \qquad b = |y_i - y_C|$$

In Fig.5, we add 21 nodes in each element to investigate the precision of the schemes. In the next section, two instances are given to test the precision of the schemes.

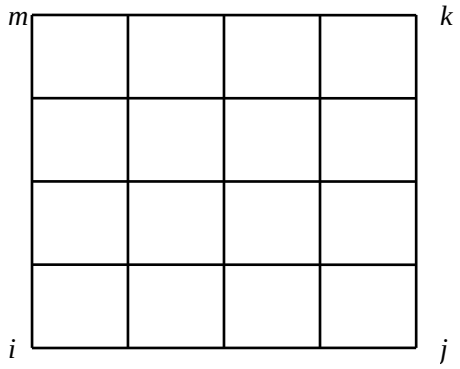

Fig. 5. Additional nodes in each element

6. Instances for Machining Simulation

6.1. Instance 1

Fig.6 shows a five-intersecting-ball surface machining simulation. The simulation results are shown in Fig.7 and Table 1. Comparing with Z-map scheme, this new scheme costs a little more time however has a much higher precision. Fig.8 shows the computational cutting marks using this new scheme.

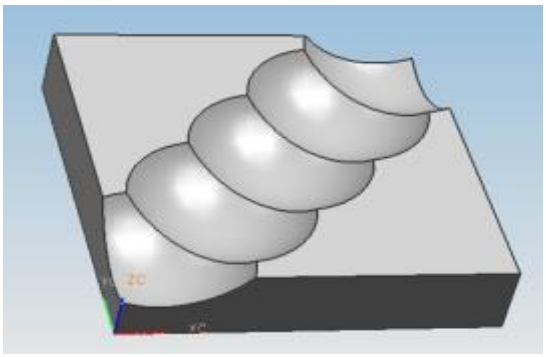

Fig. 6. Simulation instance of five-ball shape cutting

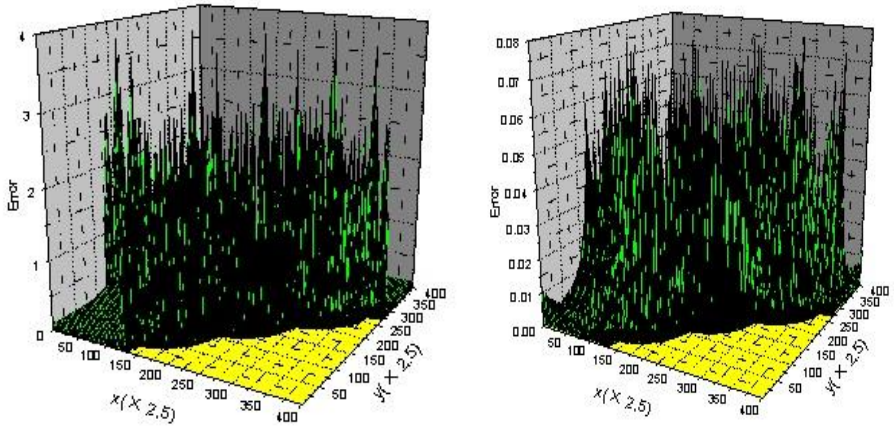

(a) (b)

Fig. 7 Errors of Z-map scheme (a) and of the new scheme (b) for 100x100 meshes

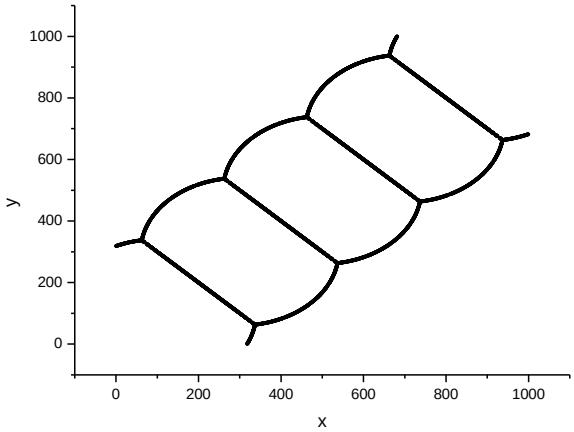

Fig. 8. Computation of cutting marks with 100×100 meshes

Table.1

Computational results of five intersecting ball surface machining simulation

	Z- map scheme		New scheme	
Mesh	100×100	1000×1000	100×100	1000×1000
Nodes	10201	1002001	10201	1002001
Parameters	10201	1002001	61206	6012006
Error	3.9	0.29	0.075	0.00012
Time cost for Computation (Sec)	0.0055	0.54	0.0059	0.58

6.2. Instance 2

Fig.9 shows a five-intersecting cylindrical surface machining simulation. The simulation results are shown in Fig.10 and Table 2. Comparing with Z-map scheme, again it shows that the new scheme costs a little more time but achieved much higher accuracy. Fig.11 shows the cutting marks determined by the new scheme.

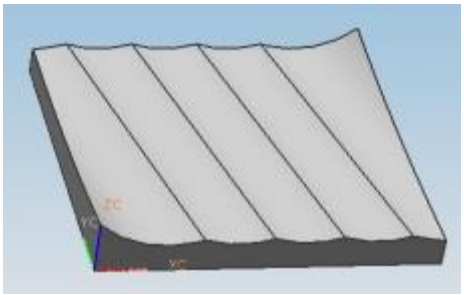

Fig. 9. Simulation instance of five-cylinder shape cutting

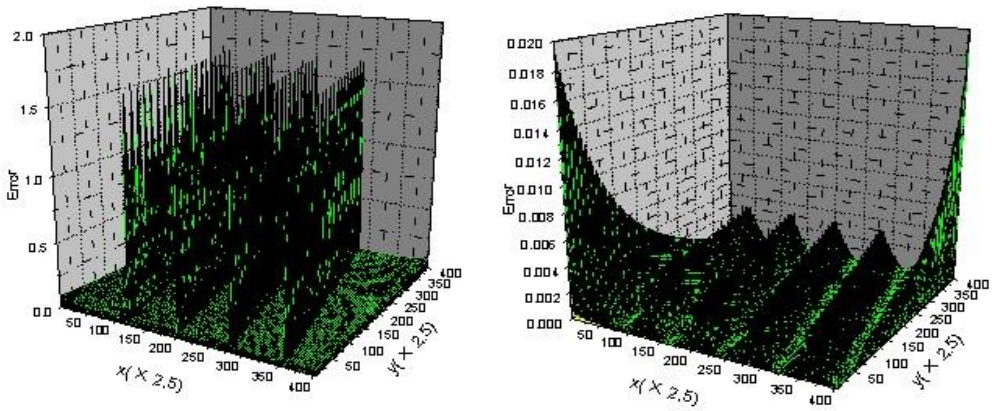

(a) (b)

Fig. 10 Errors of Z-map scheme (a) and of the new scheme (b) for 100x100 meshes

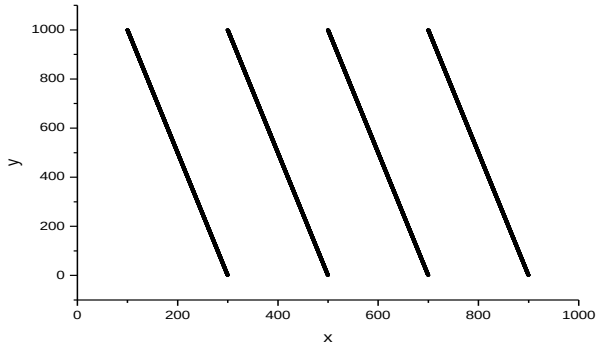

Fig. 11. Computation of cutting marks with 100×100 meshes

Table.2

Computational results of five-intersecting-cylinder surface machining simulation

	Z- map scheme		New scheme	
Mesh	100×100	1000×1000	100×100	1000×1000
Nodes	10201	1002001	10201	1002001
Parameters	10201	1002001	61206	6012006
Error	1.7	0.17	0.019	0.000020
Time cost for Computation (Sec)	0.039	3.8	0.040	3.9

7. Conclusions

The surfaces of the workpieces are composed of small smooth surfaces and cutting marks, which characterized of workpieces pattern in cutting simulations. This paper proposed a new method that uses many patch functions to describe these smooth surfaces. Besides these, more nodal parameters such as the derivatives of height functions are also used in this method. Comparison investigation shows that, comparing with other normal aligned-lines schemes, such as Z-map method, this method increases minor computational cost, but increases the simulation precision significantly. Moreover, this new method gives more detailed description for the workpiece surfaces, which is useful for the determination of cutting marks on workpieces. In the new scheme, the xy-plane is meshed into many elements, which will benefit the display of the workpieces with VRML forms while in simulation. The new modeling of workpieces might be referenced in other aligned-line based methods.

The new scheme needs derivatives of height functions determined by sweep surfaces of tools, which might bring more difficulties while facing com sophisticated tools, such as ring tools.

REFERENCES

[1]. *Yue Cai-Xu, Cai Chun-Bin, Huang Cui, et al.* Recent advances in finite element simulation of machining processes. Journal of System Simulation, 2016, 28 (4):815-825.

[2] . *Varela P I, Rakurty C S,Balaji A K,* Surface integrity in hard machining of 300m steel: effect of cutting-edge geometry on machining induced residual stresses. Procedia Cirp, 2014, 13(4):288-293.

[3]. *Hu Yan-Juan, Wang Zhan-Li, Dong Chao, et al.* The cutting force predication based on integration of symmetric fuzzy number and finite element method. Journal of Vibration, Measurement&Diagnosis, 2014, 34 (4):673-679.

[4]. *Wang Hong-Liang, Guo Rui-Feng, Peng Jian-Jun, et al.* Geometric representation of the swept volume of a generalized cutter using implicit surfaces, Journal of Mechanical Engineering, 2015,51(23):144-152.

[5]. *R Sato,* Machined Surface Simulation Techniques Considering the Motion Errors of NC Machine Tools. Journal of the Japan Society for Precision Engineering. 2017, 83 (3):204-209.

[6]. *H Li ,Z Yang ,B Xu ,C Chen ,Y Kan*.Reliability Evaluation of NC Machine Tools considering Working Conditions.Mathematical Problems in Engineering,2016 (21) :1-11.

[7] . *B. K. Choi, Y. C. Chung, and J.W. Park.* Application and extension of Z-map model. In Proc. of the 3rd Pacific Conf. on Computer Graphics and Applications, Pacific Graphics '95, 1995, p.363–382.

[8]. *Hook, T.van,* Real time shaded NC-milling display, Proc. SIGGRAPH'86 Computer Graphics, 1986, 20(4):15-20.

[9]. *Saito,T., Takahashi,T.,* NC-machining with G-buffer method, Proc. SIGGPRAPH'91, Computer Graphics, 1991, 25(4):207-216.

[10] . *Wang,W.P., Wang, K.K.,* Geometric modeling for swept column of moving solids, IEEE Computer Graphic Applications, 1986,6(12):8-17.

[11] . *Lin, Yizhen; Shen,* Yin-Lin, Enhanced virtual machining for sculptured surfaces by integrating machine tool error models into NC machining simulation, International Journal of Machine Tools and Manufacture, 2004, 44(1):79-86.

[12]. *E Uhlmann ， AJ Abackerli ,et al.* Simulation and analysis of error impact on freeform surface milling. Int J Adv Manufacture Technology, 2014, 70 (1-4):607-620.

[13]. *JixiangYang,J.R.R.Mayer*. A position independent geometric errors identification and correction method for five-axis serial machines based on screw theory. International Journal of Machine Tools & Manufacture, 2015, 95:52-66.

[14]. *Q Cheng, H Zhao, Y Zhao, B Sun, P Gu,* Machining accuracy reliability analysis of multi-axis machine tool based on Monte Carlo simulation. Journal of Intelligent Manufacturing, 2015:1-19.

[15]. *B Zhou, S Wang, C Fang, S Sun, H Dai*.Geometric error modeling and compensation for five-axis CNC gear profile grinding machine tools.International Journal of Advanced Manufacturing Technology.2017 (3):1-14.

[16]. *Cui Gangwei, Lu Yong, et al.* Geometric error compensation software system for CNC Machine tools based on NC program reconstructing. Int J Adv Manufacture Technology, 2012, 63(1-4):169-180.

[17]. *Femandez-Abia*, A I Barreiro, et al. Effect of very high cutting speeds on shearing, Cutting forces and roughness in dry turning of austenitic Stainless steels. Int J Adv Manufacture Technology, 2011, 57(1-4):61-71.

[18]. *Ana Isabel Femandez-Abia, Joaqu in Barreiro Garc ia,et al.* Estimation of Cutting Forces and Tool Wear Using Modified Mechanistic Models in High Performance Turnning.Springer,2014: 50-87.